*Article*

# Energy Efficient Transceiver Design for NOMA VLC Downlinks with Finite-Alphabet Inputs

**Zhen-Yu Wang** [ID]**, Hong-Yi Yu * and Da-Ming Wang**

National Digital Switching System Engineering and Technological Research Center, Zhengzhou 450001, China; ghostwzy@hotmail.com (Z.-Y.W.); wdm_wangdaming@163.com (D.-M.W.)
**\*** Correspondence: xxgcmaxyu@163.com; Tel.: +86-135-8989-2325

check for updates

**Abstract:** Non-orthogonal multiple access (NOMA) is considered as a promising technique in visible light communication (VLC) systems for performance enhancement. In order to improve the system's energy efficiency, we carry out transceiver design for an NOMA VLC system. We develop an optimal power allocation scheme for the system based on finite-alphabet inputs, and we propose a joint detection and decoding (JDD) algorithm for signal detection. Comprehensive simulation results demonstrate that our proposed NOMA strategy can achieve significant performance gains over the time division multiple access (TDMA) scheme, and our designed JDD algorithm outperforms the conventional successive interference cancellation (SIC) algorithm for NOMA.

**Keywords:** non-orthogonal multiple access (NOMA); visible light communication (VLC); power allocation; finite-alphabet inputs; joint detection and decoding (JDD)

## 1. Introduction

As an adjunct or alternative to radio frequency (RF) communications and as a promising technology for 5G systems, visible light communications (VLC) has become a very important area of research [1–8] due to its advantage of low cost, ultra-high bandwidth, freedom from spectral licensing issues, etc.

Considering the realistic application, the VLC systems are generally expected to support multiple users, and multiple access strategies are essential for VLC systems. Well-known orthogonal multiple access (OMA) methods such as code division multiple access (CDMA), time division multiple access (TDMA) and orthogonal frequency division multiple access (OFDMA) have been widely used to support multiuser communications. However, since different users are allocated orthogonal resources in either the code, time or frequency domain, these methods cannot provide sufficient resource reuse. In contrast to these OMA methods, a novel multiple access strategy called non-orthogonal multiple access (NOMA), which has been proposed as a promising solution for the 5G wireless networks [9–12], allows multiple users simultaneously to utilize the entire available code, time and frequency resources by multiplexing users in the power domain using superposition coding at the transmitter and successive interference cancellation (SIC) at the receiver. In VLC systems, NOMA has recently drawn great attention as an efficient solution to the limited bandwidth of light emitting diodes (LEDs) [13–15]. In [13], the performance of the NOMA VLC downlink was investigated in terms of coverage probability and ergodic sum rate, and it was verified that NOMA can achieve higher system capacity than TDMA. In [14], the authors proposed a grain ratio power allocation strategy to ensure efficiency and fairness, and it was shown that the system sum rate can be enhanced by tuning the semi-angle of LEDs and the field of view (FOV) of photodiodes (PDs). An optimal power control algorithm was proposed in [15] by using the dual method to get maximized sum logarithmic user rate. However, the above studies were mainly committed to system capacity, sum rate and user fairness, ignoring the bit error rate (BER),

which is an important index to evaluate the reliability of wireless communication systems. In addition, all the above studies utilized SIC at the receiver. As illustrated by Figure 1, the SIC-based receiver first detects one signal from the received composite signal by treating the other signals present in the same composite signal as noise. Then, the detected signal is subtracted from the received composite signal so as to detect the other signals. Since the SIC-based receiver treated the other signals as noise when detecting one signal from the same received composite signal,the SIC receiver may lead to error propagation and degrade system performance.
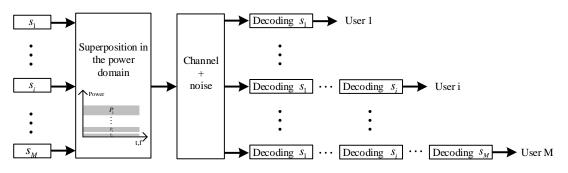


**Figure 1.** Illustration of the conventional NOMA principle.

Motivated by the aforementioned considerations, in this paper, we consider the energy-efficient transceiver design for NOMA VLC downlinks from a BER performance perspective. We develop an optimal power allocation strategy with finite-alphabet inputs for the transmitter and propose a joint detection and decoding (JDD) algorithm for the receiver. In addition, since TDMA is commonly used in the multi-user VLC system and it is easy to implement [16–19], in this paper, we choose TDMA for comparison. Comprehensive computer simulations demonstrate that our proposed NOMA strategy can achieve significant performance gains over the time division multiple access (TDMA) scheme, and our designed JDD algorithm outperforms the conventional SIC algorithm for NOMA.

The rest of this paper is organized as follows. Section 2 introduces the indoor NOMA VLC system model. Section 3 presents an optimal power allocation strategy for the transmitter and develops an efficient joint detection and decoding algorithm for the receiver. Section 4 compares the BER performance of our proposed NOMA and TDMA, as well as compares the BER performance of our proposed JDD and conventional SIC. Section 5 summarizes this paper.

## 2. System Model

As shown in Figure 2, we consider a downlink indoor NOMA VLC system with one LED and $M$ users, where the transmitter LED is located on the ceiling and the $M$ users are distributed in the same receiving plane. The LED serves $M$ users simultaneously by modulating the optical intensity according to the transmitted data. In addition, all users are equipped with a single photodiode (PD) that performs direct detection to extract the useful signal. As an initial research, we consider that the transmitted signals of this NOMA VLC system are drawn from unipolar pulse amplitude modulation (PAM) constellations, motivated by the fact that the actual transmitted signals in practical digital communication systems are drawn from finite-alphabet sets and the requirement that only nonnegative real-valued signals are allowed in VLC systems.

Unlike the conventional NOMA, which is based on SIC receiver, our proposed NOMA scheme is based on the joint detection receiver. The concept of our proposed NOMA VLC is illustrated by Figure 3, where the unipolar signals for different users are superposed in the power domain at the transmitter side and the joint detection scheme is carried out at the receiver side. According to the this NOMA VLC principle, the transmitted signals of the $M$ users, which are superposed in the power domain, are given as follows.

$$x = \sum_{i=1}^{M} p_i s_i \tag{1}$$

where $s_i \in \mathcal{S}_i = \{m\}_{m=0}^{m=2^{K_i}-1}$ is the signal intended for the $i$-th user and $p_i$ denotes the corresponding power allocation coefficient. In addition, due to the normalized total power constraint, the power allocation coefficients should satisfy $\sum_{i=1}^{M} p_i(2^{K_i} - 1) = 1$. Thus, at the receiver side, the received signal at the $m$-th user can be represented as:

$$y_m = h_m \sum_{i=1}^{M} p_i s_i + \zeta_m \tag{2}$$

where $\zeta_m$ represents additive white Gaussian noise (AWGN) with zero mean and variance $\sigma_m^2$. $h_m$ denotes the channel coefficient between the LED transmitter and $m$-th user. Since the power of the non-line-of-sight (NLOS) signals is much weaker than that of the line-of-sight (LOS) signal for VLC channels, we assume that LOS links between the transmitter and the receivers [20,21]. Then, $h_m$ is determined by:

$$h_m = \begin{cases} \frac{(\tau+1)A}{2\pi d_m^2} \cos^\tau(\phi_m) \cos(\psi_m), & 0 < \psi_m < \Psi, \\ 0, & \psi_m > \Psi. \end{cases} \tag{3}$$

where $d_m$ depicts the distance between the LED transmitter and the $m$-th user's photodiode (PD) receiver, $A$ denotes the effective PD detector area and $\Psi$ is the field-of-view angle of the PD receiver. In addition, $\phi_m$ is the angle of emergence with respect to the transmitter axis; $\psi_m$ is the angle of incidence with respect to the receiver axis; and $\tau = \frac{-ln2}{ln(\cos \Phi_{\frac{1}{2}})}$ with $\Phi_{\frac{1}{2}}$ defining the half-power angle of the LED transmitter.

Due to the low mobility of the VLC users, the channel coefficients can be easily obtained by channel estimation techniques. Thus, in this paper, we assume that the channel coefficients are available at both the transmitter and the receivers. Without loss of generality, we assume the channel coefficients have the following order:

$$h_1 \geq h_2 \geq \cdots \geq h_m \geq \cdots \geq h_M \tag{4}$$

According to the principle of NOMA that the users with worse channel conditions are allocated more power and the users with better channel conditions are allocated less power, we can get:

$$p_1 \leq p_2 \leq \cdots \leq p_m \leq \cdots \leq p_M \tag{5}$$

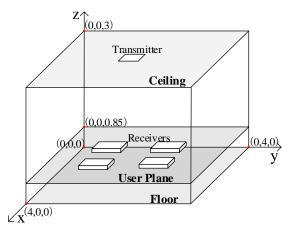In addition, the maximum likelihood (ML) detector is considered to get optimal BER performance.
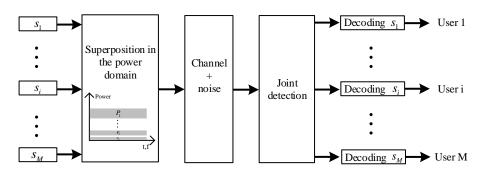


**Figure 2.** Downlink NOMA system model.

**Figure 3.** Illustration of our proposed NOMA principle.

## 3. Transceiver Design for NOMA VLC

In this section, to design an energy-efficient transceiver, we first develop an optimal power allocation strategy with unipolar PAMinputs by maximizing the minimum Euclidean distance (MED) of the received signals for signal transmission. Then, thanks to the nice structure of the received signal, we will propose a low complexity JDD algorithm for signal detection.

### 3.1. Optimal Power Allocation

This subsection aims at proposing an optimal power allocation scheme to improve the system's energy efficiency.

As we know, under high signal-to-noise ratio (SNR) conditions, the error performance of the ML detection is determined by the MED of the received signals. To optimize the performance of the ML detector, our main task is to maximize the MED between any distinct received signals under the power constraint. Hence, the corresponding problem can be stated as follows.

**Problem 1.** *For the given channel coefficient $h_i$ and any given positive integer $K_i$, find power allocation coefficients $p_i$, $i = 1, 2, \cdots, M$, such that the MED:*

$$D = \min_{(s_1 \cdots s_M) \neq (\tilde{s}_1 \cdots \tilde{s}_M), s_i, \tilde{s}_i \in \mathcal{S}_i} h_M \left| \sum_{i=1}^{M} p_i s_i - \sum_{i=1}^{M} p_i \tilde{s}_i \right| \tag{6}$$

*is maximized subject to $\sum_{i=1}^{M} p_i (2^{K_i} - 1) = 1$.*

The optimal solution to Problem 1 is determined in the following theorem.

**Theorem 1.** *Let $\check{p}_i, i = 1, 2, \cdots, M$ denote the optimal power allocation coefficient, $\check{D} = \min_{(s_1 \cdots s_M) \neq (\tilde{s}_1 \cdots \tilde{s}_M), s_i, \tilde{s}_i \in \mathcal{S}} h_M | \sum_{i=1}^{M} \check{p}_i s_i - \sum_{i=1}^{M} \check{p}_i \tilde{s}_i |$. Then, $\check{p}_i$ and $\check{D}$ can be determined in the following.*

$$\begin{cases} \check{D} = \dfrac{h_M}{2^{\sum_{j=1}^{M} K_j} - 1}, \\ \check{p}_1 = \dfrac{\check{D}}{h_M}, \check{p}_i = \dfrac{\check{D} \times 2^{\sum_{j=1}^{i-1} K_j}}{h_M}, i = 2, 3, \cdots, M. \end{cases} \tag{7}$$

The proof of Theorem 1 is postponed to Appendix A.

### 3.2. Joint Detection and Decoding Receiver Design

Intended for the optimal power allocation scheme we have proposed in the last subsection, in this subsection, we are committed to developing an efficient demodulation and decoding algorithm.

Let $\mathcal{G}_m = \{h_m \sum_{i=1}^M \check{p}_i s_i : s_i \in \mathcal{S}_i\}$. Then, according to Theorem 1, we can obtain that $\frac{h_M \mathcal{G}_m}{h_m \check{D}} = \{\frac{h_M}{\check{D}} \sum_{i=1}^M \check{p}_i s_i : s_i \in \mathcal{S}_i\} = \{m\}_{m=0}^{m=2^{\sum_{j=1}^M K_j} - 1}$ is a $2^{\sum_{j=1}^M K_j}$-ary equally-spaced PAM constellation. In this context, the following low-complexity JDD algorithm can be utilized for signal detection.

**Algorithm 1.** *(Joint detection and decoding (JDD)) Given the received signals $y_m$ denoted by (2), the optimal ML estimate of the sum signal $g_m \in \mathcal{G}_m$ can be attained by:*

$$\hat{g}_m = \frac{h_m \check{D}}{h_M} \begin{cases} 0, & \frac{h_M y_m}{h_m \check{D}} \leq 0 \\ \lfloor \frac{h_M y_m}{h_m \check{D}} + \frac{1}{2} \rfloor, & 0 < \frac{h_M y_m}{h_m \check{D}} \leq 2^{\sum_{j=1}^M K_j} - 1 \\ 2^{\sum_{j=1}^M K_j} - 1, & \frac{h_M y_m}{h_m \check{D}} > 2^{\sum_{j=1}^M K_j} - 1. \end{cases}$$

*Then, the estimate signal $\hat{s}_{mi}$ of $s_i$ at user $m$ is given as follows.*

$$\begin{cases} \hat{s}_{m1} = \frac{h_M \hat{g}_m}{h_m \check{D}} mod 2^{K_1}, \\ \hat{s}_{mi} = \frac{\frac{h_M \hat{g}_m}{h_m \check{D}} - \frac{h_M \hat{g}_m}{h_m \check{D}} mod 2^{\sum_{j=1}^{i-1} K_j}}{2^{\sum_{j=1}^{i-1} K_j}} mod 2^{K_i}, i \geq 2. \end{cases}$$

From Algorithm 1, we can observe that our proposed JDD algorithm treats all the signals as useful information, which is different from SIC, which treats other signals as noise when detecting. In addition, we can get that the overall complexity of our proposed JDD algorithm is $O(\sum_{j=1}^{i-1} K_j)$, and it is lower than the traditional ML-based SIC algorithm with complexity $O(2^{\sum_{j=1}^i K_j})$ [22].

## 4. Simulations

In this section, we evaluate the performance of our proposed transceiver design for the NOMA VLC system by comprehensive computer simulations.

As illustrated by Figure 2, we carry out the simulations in a $4.0\,\text{m} \times 4.0\,\text{m} \times 3.0\,\text{m}$ room for an indoor environment; the transmitter LED is located at $(2.0\,\text{m}, 2.0\,\text{m}, 3.0\,\text{m})$; and all the users are located at a plane with a height of $0.85\,\text{m}$, which is denoted by user plane. Some other key system parameters are shown in Table 1. The channel coefficient of each channel realization can be computed based on (3) and normalized by being divided by the maximum channel coefficient. The SNR is defined by $\frac{1}{\sigma^2}$ for the normalized peak optical power. In addition, to make all the comparisons fair, the ML demodulator is adopted by all schemes. More details of our computer simulations are given as follows.

**Table 1.** Key system parameters.

| Parameter | Value |
| --- | --- |
| Room size | $4.0\,\text{m} \times 4.0\,\text{m} \times 3.0\,\text{m}$ |
| LED coordinate | $(2.0\,\text{m}, 2.0\,\text{m}, 3.0\,\text{m})$ |
| PD detector area | $A = 1\,\text{cm}^2$ |
| Field-of-view angle | $60°$ |
| Half-power angle | $60°$ |
| Height of receiver plane | $0.85\,\text{m}$ |

We first compare the average BER performance of our proposed NOMA scheme and the conventionally used TDMA. The transmitted signals of the two schemes are shown in Table 2, and we consider that all the users are randomly distributed on the user plane, as illustrated in Figure 2. We randomly select 20 user groups to simulate their average BER performance, and the simulation results for two, three or four users per user group are shown in Figures 4–6, respectively. From these

figures, we can get that our proposed NOMA scheme significantly outperforms the conventionally used TDMA. For example, the average gain of our proposed NOMA scheme over TDMA at the error rate of $10^{-5}$ is about 7 dB for $M = 2, K_1 = 1, K_2 = 3$. The main reason for this is that the error performance is dominated by the MED of the received constellation, and the ratio of MED of our proposed NOMA and TDMA is determined by:

$$20\log_{10}\left(\frac{h_M}{M(2^{\sum_{j=1}^{M} K_j} - 1)}\right) / \left(\frac{h_M}{\sum_{i=1}^{M} 2^{MK_i} - M}\right) = 20\log_{10}\frac{\sum_{i=1}^{M} 2^{MK_i} - M}{M(2^{\sum_{j=1}^{M} K_j} - 1)} \tag{8}$$

Then, for $M = 2, K_1 = 1, K_2 = 3$, the obtained gain of our proposed NOMA over TDMA is given by $20\log_{10}\frac{2^{2K_1}+2^{2K_2}-2}{2(2^{K_1+K_2}-1)} = 20\log_{10}\frac{2^{2\times1}+2^{2\times3}-2}{2(2^{1+3}-1)} \approx 6.85$ dB, which is consistent with the simulation results in Figure 4. In addition, we simulate the average BER performance of our proposed NOMA scheme with different transmitter LED position, and the simulation results are illustrated in Figure 7. From this figure, we can see that no matter where the transmitter LED is, our proposed design has a good performance over TDMA.

Furthermore, we also compare the average BER performance of our proposed JDD algorithm and the conventional SIC algorithm. As illustrated by Figure 4, our proposed JDD algorithm outperforms the SIC algorithm. For example, the obtained gain of the JDD algorithm compared to the SIC algorithm is about 5 dB for $M = 2, K_1 = 2, K_2 = 3$.

As illustrated in the above simulations, our proposed transceiver design for NOMA significantly outperforms SIC-based NOMA and TDMA. Using our proposed NOMA-JDD scheme, we can achieve higher rates of data transmission than using TDMA or NOMA-SIC with the same BER and SNR.
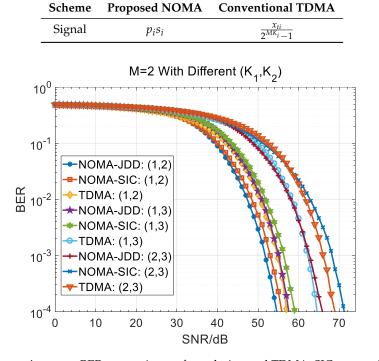
**Table 2.** The transmitted signal of the two schemes.

| Scheme | Proposed NOMA | Conventional TDMA |
|---|---|---|
| Signal | $p_i s_i$ | $\frac{x_{ti}}{2^{MK_i}-1}$ |



**Figure 4.** Two users' average BER comparisons of our design and TDMA. SIC, successive interference cancellation.

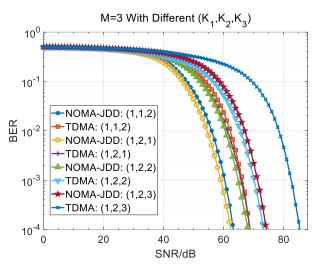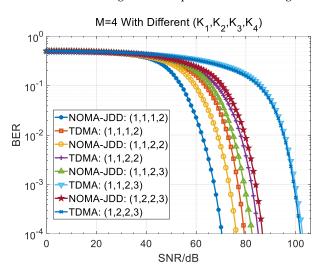**Figure 5.** Three users' average BER comparisons of our design and TDMA.



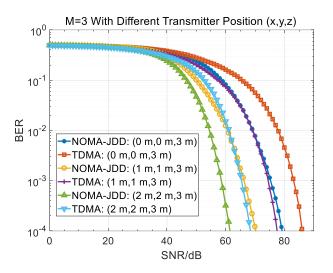**Figure 6.** Four users' average BER comparisons of our design and TDMA.



**Figure 7.** Three users' average BER comparisons of our design and TDMA with $K_1 = 1, K_2 = 2, K_3 = 1$ for different transmitter positions.

## 5. Conclusions

In this paper, we have designed the transceiver for an indoor NOMA VLC system to enhance the system's energy efficiency. For the transmitter, we have proposed an optimal power allocation scheme by maximizing the MED of the received signal, and for the receiver, we have developed a low-complexity and reliable JDD algorithm. The simulation results have demonstrated that our proposed NOMA scheme significant outperforms TDMA, and our designed JDD algorithm can achieve higher detection accuracy than the conventionally used SIC algorithm.

**Author Contributions:** Z.-Y.W. has contributed to the scientific part of this work. Z.-Y.W. and H.-Y.Y. contributed to the conception and design of the study. D.-M.W. has critically reviewed the paper. All authors have read and approved the final manuscript.

**Conflicts of Interest:** The authors declare no conflicts of interest.

## Appendix A

**Proof of Theorem 1.** We need to establish the following two propositions to prove Theorem 1.

**Proposition A1.** *For any M positive real-valued numbers $p_i$ and positive integers $K_i$, if $0 \leq p_1 \leq p_2 \leq \cdots \leq p_M$ and $D > 0$, then, we have $h_M p_1 \geq D$ and $h_M p_i \geq D \times 2^{\sum_{j=1}^{i-1} K_j}$ for $2 \leq i \leq M$.*

**Proof of Proposition A1:** Let $\mathcal{G}_M = \{h_M \sum_{i=1}^{M} p_i s_i : s_i \in \mathcal{S}_i\}$. Since $D > 0$, we can rearrange all the $2^{\sum_{j=1}^{M} K_j}$ elements of $\mathcal{G}_M$ in a strictly increasing order such that $g_0 < g_1 < \cdots < g_{2^{\sum_{j=1}^{M} K_j} - 1}$. Now, it is more clear to see that if we reduce the power of $\mathcal{S}_i$ such that $g_k = kD$, then $\min_{g \neq \tilde{g}, g, \tilde{g} \in \tilde{\mathcal{G}}_M} |g - \tilde{g}| = \min_{g \neq \tilde{g}, g, \tilde{g} \in \mathcal{G}_M} |g - \tilde{g}| = D$, where $\tilde{\mathcal{G}}_M = \{h_M \sum_{i=1}^{M} \tilde{p}_i s_i : s_i \in \mathcal{S}_i\} = \{kD\}_{k=0}^{k=2^{\sum_{j=1}^{M} K_j} - 1}$, and the consumed peak power of each user for $\tilde{\mathcal{G}}_M$ is not larger than that for $\mathcal{G}_M$. In addition, it holds that $p_i \geq \tilde{p}_i$ for $1 \leq i \leq M$. Then, according to Proposition A1 in [23], if we let $\mathcal{X}_i = \{h_M \tilde{p}_i k_i : k_i \in \{k\}_{k=0}^{k=2^{K_i} - 1}\}, 0 \leq \tilde{p}_1 \leq \tilde{p}_2 \leq \cdots \leq \tilde{p}_M$ and $\{h_M \sum_{i=1}^{M} \tilde{p}_i k_i : k_i \in \{k\}_{k=0}^{k=2^{K_i} - 1}\} = \{D \times k\}_{k=0}^{k=2^{\sum_{i=1}^{M} K_i} - 1}$, then we have $\{h_M \tilde{p}_1 k : k \in \{k\}_{k=0}^{k=2^{K_1} - 1}\} = \{D \times k\}_{k=0}^{k=2^{K_1} - 1}$ and $\{h_M \tilde{p}_i k : k \in \{k\}_{k=0}^{k=2^{K_i} - 1}\} = \{D \times k \times 2^{\sum_{j=1}^{i-1} K_j}\}_{k=0}^{k=2^{K_i} - 1}$ for $2 \leq i \leq M$, i.e., $h_M \tilde{p}_1 = D$ and $h_M \tilde{p}_u = D \times 2^{\sum_{j=1}^{i-1} K_j}$ for $2 \leq i \leq U$. Therefore, it indeed holds that $h_M p_1 \geq h_M \tilde{p}_1 = D$ and $h_M p_i \geq h_M \tilde{p}_i = D \times 2^{\sum_{j=1}^{i-1} K_j}$ for $2 \leq i \leq M$, and the proof of Proposition A1 is complete.　□

**Proposition A2.** *For any given minimum Euclidean distance D, if $h_M p_1 \geq D$, $h_M p_i \geq D \times 2^{\sum_{j=1}^{i-1} K_j}$ for $2 \leq i \leq M$ and $\sum_{i=1}^{M} p_i (2^{K_i} - 1) = 1$, then we have $D \leq \check{D}$.*

**Proof of Proposition A2:** To prove it by contradiction, we assume that under the condition that $h_M p_1 \geq D$, $h_M p_i \geq D \times 2^{\sum_{j=1}^{i-1} K_j}$ for $2 \leq i \leq M$ and $\sum_{i=1}^{M} p_i (2^{K_i} - 1) = 1$, there exists at least one D such that $D > \check{D}$. Then, we can get that $h_M p_1 > \check{D}$ and $h_M p_i > \check{D} \times 2^{\sum_{j=1}^{i-1} K_j}$ for $2 \leq i \leq M$, and thus, we have:

$$h_M \sum_{i=1}^{M} p_i (2^{K_i} - 1) > \quad \check{D}(2^{K_1} - 1) + \sum_{i=2}^{M} \check{D} \times 2^{\sum_{j=1}^{i-1} K_j} (2^{K_i} - 1) = \quad \check{D}(2^{\sum_{j=1}^{M} K_j} - 1) \qquad \text{(A1)}$$

Then, combing this result with $\check{D} = \dfrac{h_M}{2^{\sum_{j=1}^{M} K_j} - 1}$ in Theorem 1, we can obtain that $\sum_{i=1}^{M} p_i (2^{K_i} - 1) > 1$, which contradicts the condition $\sum_{i=1}^{M} p_i (2^{K_i} - 1) = 1$, and thus, our assumption is

not true. In addition, we can find that if and only if $h_M p_1 = D$ and $h_M p_i = D \times 2^{\sum_{j=1}^{i-1} K_j}$ for $2 \le i \le M$, we have $D = \check{D}$. This completes the proof of Proposition A2. $\square$

Then, according to Proposition A2, we have $\check{D} = \frac{h_M}{2^{\sum_{j=1}^{M} K_j} - 1}$, $\check{p}_1 = \frac{\check{D}}{h_M}$ and $\check{p}_i = \frac{\check{D} \times 2^{\sum_{j=1}^{i-1} K_j}}{h_M}$ for $i = 2, 3, \cdots, M$. Therefore, the proof of Theorem 1 is complete. $\square$

## References

1. O'Brien, D.C.; Zeng, L.; Le-Minh, H.; Faulkner, G.; Walewski, J.W.; Randel, S. Visible light communications: Challenges and possibilities. In Proceedings of the 2008 IEEE 19th International Symposium on Personal, Indoor and Mobile Radio Communications, Cannes, France, 15–18 September 2008; pp. 1–5.
2. Haruyama, S. Visible light communications. In Proceedings of the 36th European Conference and Exhibition on Optical Communication, Torino, Italy, 19–23 September 2010; pp. 1–22.
3. Elgala, H.; Mesleh, R.; Haas, H. Indoor optical wireless communication: Potential and state-of-the-art. *IEEE Commun. Mag.* **2011**, *49*, 56–62. [CrossRef]
4. Jovicic, A.; Li, J.; Richardson, T. Visible light communication: opportunities, challenges and the path to market. *IEEE Commun. Mag.* **2013**, *51*, 26–32. [CrossRef]
5. Gancarz, J.; Elgala, H.; Little, T.D.C. Impact of lighting requirements on vlc systems. *IEEE Commun. Mag.* **2013**, *51*, 34–41. [CrossRef]
6. Cogalan, T.; Haas, H. Why would 5G need optical wireless communications. In Proceedings of the 2017 IEEE 28th Annual International Symposium on Personal, Indoor, and Mobile Radio Communications (PIMRC), Montreal, QC, Canada, 8–13 October 2017; pp. 1–6.
7. Pešek, P.; Zvanovec, S.; Chvojka, P.; Bhatnagar, M.R.; Ghassemlooy, Z.; Saxena, P. Mobile User Connectivity in Relay-Assisted Visible Light Communications. *Sensors* **2018**, *18*, 1125. [CrossRef] [PubMed]
8. Wang, Z.Y.; Yu, H.Y.; Zhang, Y.Y.; Wang, D.M. Optimization of Finite-Alphabet Signaling for Two-User Multiaccess VLC Systems. *IEEE Photonics J.* **2018**, *10*. [CrossRef]
9. Saito, Y.; Kishiyama, Y.; Benjebbour, A.; Nakamura, T.; Li, A.; Higuchi, K. Non-Orthogonal Multiple Access (NOMA) for Cellular Future Radio Access. In Proceedings of the 2013 IEEE 77th Vehicular Technology Conference (VTC Spring), Dresden, Germany, 2–5 June 2013; pp. 1–5.
10. Saito, Y.; Benjebbour, A.; Kishiyama, Y.; Nakamura, T. System-level performance evaluation of downlink non-orthogonal multiple access (NOMA). In Proceedings of the 2013 IEEE 24th Annual International Symposium on Personal, Indoor, and Mobile Radio Communications (PIMRC), London, UK, 8–11 September 2013; pp. 611–615.
11. Ding, Z.; Yang, Z.; Fan, P.; Poor, H.V. On the performance of non-orthogonal multiple access in 5G systems with randomly deployed users. *IEEE Signal Process. Lett.* **2014**, *21*, 1501–1505. [CrossRef]
12. Benjebbour, A.; Saito, Y.; Kishiyama, Y.; Li, A.; Harada, A.; Nakamura, T. Concept and practical considerations of non-orthogonal multiple access (NOMA) for future radio access. In Proceedings of the 2013 International Symposium on Intelligent Signal Processing and Communication Systems, Okinawa, Japan, 12–15 November 2013; pp. 770–774.
13. Yin, L.; Wu, X.; Haas, H. On the performance of non-orthogonal multiple access in visible light communication. In Proceedings of the 2015 IEEE 26th Annual International Symposium on Personal, Indoor, and Mobile Radio Communications (PIMRC), Hong Kong, China, 30 August–2 September 2015; pp. 1354–1359.
14. Marshoud, H.; Kapinas, V.M.; Karagiannidis, G.K.; Muhaidat, S. Non-orthogonal multiple access for visible light communications. *IEEE Photonics Technol. Lett.* **2016**, *28*, 51–54. [CrossRef]
15. Yang, Z.; Xu, W.; Li, Y. Fair non-orthogonal multiple access for visible light communication downlinks. *IEEE Wirel. Commun. Lett.* **2017**, *6*, 66–69. [CrossRef]
16. Zhang, Y.Y.; Yu, H.Y.; Zhang, J.K. Block precoding for peak-limited MISO broadcast VLC: Constellation-optimal structure and addition-unique designs. *IEEE J. Sel. Areas Commun.* **2018**, *36*, 78–90. [CrossRef]
17. Zhu, Y.J.; Wang, W.Y.; Xin, G. Faster-than-nyquist signal design for multiuser multicell indoor visible light communications. *IEEE Photonics J.* **2017**, *8*, 1–12. [CrossRef]

18.  Zhang, Y.Y.; Yu, H.Y.; Zhang, J.K.; Zhu, Y.J. Signal-cooperative multilayer-modulated VLC systems for automotive applications. *IEEE Photonics J.* **2016**, *8*, 1–9. [CrossRef]

19.  Kim, S.M.; Baek, M.W.; Nahm, S.H. Visible light communication using TDMA optical beamforming. *EURASIP J. Wirel. Commun. Netw.* **2017**, *2017*, 56. [CrossRef]

20.  Kahn, J.M.; Barry, J.R. Wireless infrared communications. *Proc. IEEE* **1997**, *85*, 265–298. [CrossRef]

21.  Shen, H.; Wu, Y.F.; Xu, W.; Zhao, C.M. Optimal power allocation for downlink two-user non-orthogonal multiple access in visible light communication. *J. Commun. Inf. Netw.* **2017**, *2*, 57–64. [CrossRef]

22.  Zhu, Y.J.; Liang, W.F.; Wang, C.; Wang, W.Y. Energy-efficient constellations design and fast decoding for space-collaborative MIMO visible light communications. *Opt. Commun.* **2017**, *38*, 260–273. [CrossRef]

23.  Zhang, Y.Y.; Zhang, J.K.; Yu, H.Y. Physically securing energy-based massive MIMO MAC via joint alignment of multi-user constellations and artificial noise. *IEEE J. Sel. Areas Commun.* **2018**, *36*, 829–844. [CrossRef]